2720 *Chem. Mater.* **2010,** *22,* 2720–2729
DOI:10.1021/cm903048u

CHEMISTRY OF MATERIALS
Article

Novel Periphery-Functionalized Solvatochromic Nitrostilbenes As Precursors for Class II Hybrid Materials

Katja Schreiter,[†] Katja Hofmann,[†] Andreas Seifert,[†] Alexander Oehlke,[†] Katharina Ladewig,[†] Tobias Rüffer,[‡] Heinrich Lang,[‡] and Stefan Spange*[,†]

[†]*Department of Polymer Chemistry and* [‡]*Department of Inorganic Chemistry, Institute of Chemistry, Chemnitz University of Technology, Strasse der Nationen 62, 09111 Chemnitz, Germany*

Received October 1, 2009. Revised Manuscript Received March 25, 2010

Novel donor−acceptor-substituted stilbenes were synthesized by means of nucleophilic aromatic substitution starting from 1-fluoro-2-nitro-4-[(*E*)-2-(4-nitrophenyl)vinyl]benzene and *n*-propylamine, L-proline, and 2-aminopropane-1,3-diol as model compounds for the study of molecular interactions in the solid-state and liquid environments of different polarity. The solvatochromic behavior of the chromophoric building blocks has been studied and interpreted using the empirical Kamlet−Taft solvent parameters π^* (dipolarity/polarizability), α (hydrogen bond donating capacity), and β (hydrogen bond accepting ability) in terms of the well-established linear solvation energy relationship (LSER): $\nu_{max} = \nu_{max,0} + s\pi^* + a\alpha + b\beta$. The most dominant effect on the solvatochromic behavior of nitrostilbenes is caused by interactions with solvents of different polarity/polarizability. To evaluate the environmental effects the nitrostilbenes are subjected to, we also investigated the UV/vis spectroscopic behavior as pure crystal powders and as an organic component in class II xerogels. Starting from these chromophores we were able to use three different synthetic routes in order to bind the chromophore covalently to the trialkoxysilane via an amine, amide or urethane function, respectively. The precursors thus obtained were converted into the corresponding xerogels in situ in a one-pot procedure. Two routes can be followed−one involving incorporation of the chromophore in the main chain, and the other involving incorporation in the side chain. All obtained organic−inorganic hybrid materials were characterized in detail using solid-state NMR, FT-IR, and UV/vis spectroscopy.

1. Introduction

Sol−gel processes have been investigated extensively[1] and are well established in materials science[2−4] and catalysis.[5−8] Completely new perspectives for the synthesis and structural design of complex hybrid materials have been opened up and the combination of specific properties of organic functional groups with those of a silicate network has been made possible on a molecular level.[9−16] Consequently, there is a significant potential for application in organometallic catalysis,[17] sensors,[18] and for photo-optic[19,20] and nonlinear optical (NLO) materials.[21−24] Most recently chiral sol−gel materials[17,25,26] have been developed, for example, by the entrapment of chiral molecules in a silica matrix. This concept has been applied successfully to a large number of

*Corresponding author. E-mail: stefan.spange@chemie.tu-chemnitz.de.

(1) Hench, L. L.; West, J. K. *Chem. Rev.* **1990**, *90*, 33–72.
(2) Philipp, G.; Schmidt, H. *J. Non-Cryst. Solids* **1984**, *63*, 283–92.
(3) Boury, B.; Corriu, R. J. P. *Adv. Mater.* **2000**, *12*, 989–992.
(4) Novak, B. M. *Adv. Mater.* **1993**, *5*, 422–433.
(5) Lu, Z.-I.; Lindner, E.; Mayer, H. A. *Chem. Rev.* **2002**, *102*, 3543–3578.
(6) Kingsbury, J. S.; Garber, S. B.; Giftos, J. M.; Gray, B. L.; Okamoto, M. M.; Farrer, R. A.; Fourkas, J. T.; Hoveyda, A. H. *Angew. Chem.* **2001**, *113*, 4381–4386.
(7) Elias, X.; Pleixats, R.; Man, M. W. C.; Moreau, J. J. E. *Adv. Synth. Catal.* **2007**, *349*, 1701–1713.
(8) Adima, A.; Moreau, J. J. E.; Man, M. W. C. *Chirality* **2000**, *12*, 411–420.
(9) Judeinstein, P.; Sanchez, C. *J. Mater. Chem.* **1996**, *6*, 511–525.
(10) Corriu, R. J. P.; Mehdi, A.; Reyé, C. *J. Mater. Chem.* **2005**, *15*, 4285–4294.
(11) Corriu, R. J. P. *Angew. Chem., Int. Ed.* **2000**, *39*, 1376–1398.
(12) Corriu, R. *Polyhedron* **1998**, *17*, 925–934.
(13) Moreau, J. J. E.; Pichon, B. P.; Man, M. W. C.; Bied, C.; Pritzkow, H.; Bantignies, J.-L.; Dieudonné; Sauvajol, J.-L. *Angew. Chem., Int. Ed.* **2004**, *43*, 203–206.
(14) Wen, J.; Wilkes, G. L. *Chem. Mater.* **1996**, *8*, 1667–1681.
(15) Spange, S.; Seifert, A.; Müller, H.; Hesse, S.; Jäger, C. *Angew. Chem., Int. Ed.* **2002**, *41*, 1729–1732.
(16) Corriu, R.; Leclercq, D. *Angew. Chem., Int. Ed.* **1996**, *35*, 1420–1436.
(17) Defreese, J. L.; Katz, A. *Chem. Mater.* **2005**, *17*, 6503–6506.
(18) García-Acosta, B.; Comes, M.; Bricks, J. L.; Kudinova, M. A.; Kurdyukov, V. V.; Tolmachev, A. I.; Descalzo, A. B.; Marcos, M. D.; Martínez-Máñez, R.; Moreno, A.; Sancenón, F.; Soto, J.; Villaescusa, L. A.; Rurack, K.; Barat, J. M.; Escriche, I.; Amorós, P. *Chem. Commun.* **2006**, 2239–2241.
(19) Levy, D.; Avnir, D. *J. Phys. Chem.* **1988**, *92*, 4734–4738.
(20) Li, H.; Lin, N.; Wang, Y.; Feng, Y.; Gan, Q.; Zhang, H.; Dong, Q.; Chen, Y. *Eur. J. Inorg. Chem.* **2009**, 519–523.
(21) Chaumel, F.; Jiang, H.; Kakkar, A. *Chem. Mater.* **2001**, *13*, 3389–3395.
(22) Oviatt, H. W., Jr.; Shea, K. J. *Chem. Mater.* **1995**, *7*, 493–498.
(23) Yang, Z.; Xu, C.; Wu, B.; Dalton, L. R. *Chem. Mater.* **1994**, *6*, 1899–1901.
(24) Nosaka, Y.; Tohriiwa, N.; Kobayashi, T.; Fujii, N. *Chem. Mater.* **1993**, *5*, 930–932.
(25) Marx, S.; Avnir, D. *Acc. Chem. Res.* **2007**, *40*, 768–776.
(26) Adima, A.; Moreau, J. J. E.; Man, M. W. C. *Chirality* **2000**, *12*, 411–420.
(27) Arrachart, G.; Carcel, C.; Moreau, J. J. E.; Hartmeyer, G.; Alonso, B.; Massiot, D.; Creff, G.; Bantignies, J.-L.; Dieudonne, P.; Man, M. W. C.; Althoff, G.; Babonneau, F.; Bonhomme, C. *J. Mater. Chem.* **2008**, *18*, 392–399.

Published on Web 04/06/2010

organic compounds and biomolecules, e.g., amino acids, sugars, enzymes, antibodies, surfactants, and chiral polymers.[25,27] Organic functional moieties can be incorporated into the silica network in various ways. On the one hand, chromophoric molecules can be held in an inorganic network by weak interactions like van der Waals forces or hydrogen bonds (class I, host−guest concept).[9,28,29] On the other hand, it is possible to bind the chromophore to the matrix directly by one or more covalent bonds (class II).[9,28,29]

Functional stilbenes have gained wide interest and found a vast range of useful applications in the areas of optical switching, image storage devices, and molecular function regulation and are thus interesting chromophores as organic component in organic−inorganic hybrid materials.[30,31] The sol−gel technique represents an attractive means of synthesizing materials which ensure the excellent chemical stability of their chromophoric systems. Through the incorporation of chromophores into a silica matrix, these materials are predestined for pigment applications.[32] With regard to this and other potential applications, it is important to know whether and how the nitrostilbene unit interacts with its surroundings (e.g., self-interaction, interaction with environment). The probing of dye aggregates and supramolecular structures by means of UV/vis spectroscopy is an experimental challenge and of importance for both academic research and practical application in nanoscience technology. For this objective, the exact knowledge of the solid-state structures is necessary, and the respective UV/vis spectra have to be significantly different as a function of structure variation. This issue requires the choice of a suitable model systems that show color changes as a function of the nature of accumulation processes. Nitrostilbenes shows sufficient solvatochromic and crystallochromic effects depending on structure variation and environmental influences. In this context, we here report novel amino acid- and diol-functionalized nitrostilbenes **2** and **3**, which can be synthesized from fluorinated nitrostilbene **1**.[33,34] A specific object is the study of solvent influence on the UV/vis absorption spectra of these aminonitrostilbenes.

Interactions of solvatochromic dyes with pure solvents or solvent mixtures arise from a combination of many

Scheme 1. Combination of Nucleophilic Aromatic Substitution and Sol−Gel Process in a One-Pot (X = F, OCH_3) and Two-Step Synthesis (n = 1, 2) Opens the Possibility of Producing Chromophoric Class II Hybrid Materials

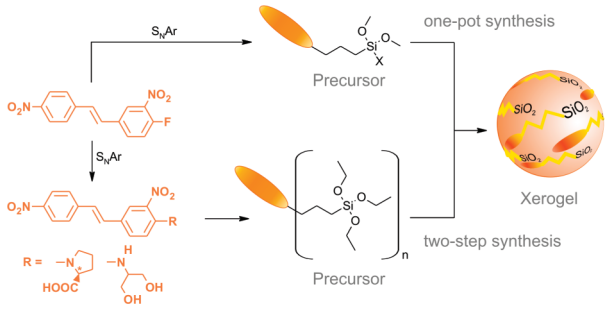

effects.[35−40] Multiple intermolecular solute/solvent interactions can be described using linear free energy relationships (LSER).[35,36] To separate the effects of nonspecific chemical interactions including electrostatic effects (dipolarity/polarizability) from specific interactions (hydrogen bonding), we used the simplified Kamlet−Taft equation (eq 1)[41−45]

$$\tilde{\nu}_{\max} = \tilde{\nu}_{\max,0} + a\alpha + b\beta + s\pi^* \qquad (1)$$

Using eq 1, the effect of hydrogen bonding donor capacity (HBD) α,[41] the hydrogen bonding acceptor capacity (HBA) β,[42] and the dipolarity/polarizability π^*[43,44] of a solvent can be expressed. $\tilde{\nu}_{\max,0}$ corresponds to a standard process, referenced to a nonpolar medium. a, b, and s represent solvent-independent correlation coefficients, which reflect the effect of each parameter.

A complementary point of investigations is the study of environmental effects in the solid state. Therefore, functionalization with fluorine (**1**), amino acid (**2**), and diol substituents (**3**) allows reaction with trialkoxysilanes to give the chromophoric trialkoxysilanes **1-PR**−**3-PR** (precursor), which can be converted into organically modified class II silica gel (**1-XG**−**3-XG**) by addition of tetraethoxysilane in a sol−gel process (Scheme 1). The properties of the organic−inorganic hybrid materials can be discussed in context of the results obtained from studies of solvatochromism.

In the present paper, the properties of these amino nitrostilbenes were investigated in solution (solvatochromism in terms of Kamlet and Taft), in the solid state (X-ray diffraction), and after embedding into a silica matrix (^{13}C-CP-MAS NMR, ^{29}Si-CP-MAS NMR, thermogravimetric measurements, FT-IR, UV/vis spectroscopy).

2. Experimental Section

General Remarks. Solvents from Merck, Fluka, Lancaster, and Aldrich were redistilled over appropriate drying agents prior to use. All commercial reagents were used without further

(28) Chaumel, F.; Jiang, H.; Kakkar, A. *Chem. Mater.* **2001**, *13*, 3389–3395.
(29) Pandey, S.; Baker, G. A.; Kane, M. A.; Bonzagni, N. J.; Bright, F. V. *Chem. Mater.* **2000**, *12*, 3547–3551.
(30) Wolf, M. O.; Fox, M. A. *Langmuir* **1996**, *12*, 955–962.
(31) Marten, J.; Erbe, A.; Critchley, K.; Bramble, J. P.; Weber, E.; Evans, S. D. *Langmuir* **2008**, *24*, 2479–2486.
(32) Seifert, A.; Ladewig, K.; Schönherr, P.; Hofmann, K.; Lungwitz, R.; Roth, I; Pohlers, A.; Hoyer, W.; Baumann, G.; Schulze, S.; Hietschold, M.; Moszner, N.; Burtscher, P.; Spange, S. *J. Sol−Gel Sci. Technol.* **2010**, *53*, 328–341.
(33) Jourdant, A.; González-Zamora, E.; Zhu, J. *J. Org. Chem.* **2002**, *67*, 3163–3164.
(34) Roth, I.; Simon, F.; Bellmann, C.; Seifert, A.; Spange, S. *Chem. Mater.* **2006**, *18*, 4730–4739.
(35) Reichardt, C. In *Solvents and Solvent Effects in Organic Chemistry*, 2nd ed.; VCH: Weinheim, Germany, 1988, and references therein.
(36) Reichardt, C. *Chem. Rev.* **1994**, *94*, 2319–2358.
(37) Müller, P. *Pure Appl. Chem.* **1994**, *66*, 1077–1079.
(38) Marcus, Y. *Chem. Soc. Rev.* **1993**, *22*, 409–416.
(39) Gutmann, V. *Coord. Chem. Rev.* **1976**, *18*, 225–240.
(40) Gutmann, V. *The Donor−Acceptor Approach to Molecular Interactions*; Plenum Press: New York, 1978.
(41) Taft, R. W.; Kamlet, M. J. *J. Am. Chem. Soc.* **1976**, *98*, 2886–2894.
(42) Kamlet, M. J.; Taft, R. W *J. Am. Chem. Soc.* **1976**, *98*, 377–383.
(43) Kamlet, M. J.; Hall, T. N.; Boykin, J.; Taft, R. W. *J. Org. Chem.* **1979**, *44*, 2599–2604.
(44) Kamlet, M. J.; Abboud, J. L. M.; Taft, R. W. *J. Am. Chem. Soc.* **1977**, *99*, 6027–6038.
(45) Kamlet, M. J.; Abboud, J.-L. M.; Abraham, M. H.; Taft, R. W. *J. Org. Chem.* **1983**, *48*, 2877–2887.

purification, and were purchased from the following supplier: Merck: L(−)-proline (≥99%); 2-aminopropane-1,3-diol (97%). Compound **1** was prepared as described in the literature.[33,34]

All melting points (Mp) were measured on a Boetius melting point apparatus and were uncorrected. The thermogravimetric measurements were performed in a helium atmosphere with a 10 K/min heating rate (temperature range: 30−800 °C) using a Thermogravimetric Analyzer 7 (Perkin-Elmer). The UV/vis absorption spectra were obtained with an MCS 400 diode array UV/vis spectrometer from Carl Zeiss, Jena, connected via glass-fiber optics. Specific surface area Nitrogen adsorption isotherms were measured at 77.6 K using Areameter II setup from Ströhlein Instruments.

^{1}H NMR and ^{13}C NMR spectra were measured at 20 °C on a Bruker Avance 250 NMR spectrometer at 250 and 69.9 MHz. The residual solvent signals (DMSO-d_6) were used as internal standards. The solid-state ^{13}C-{^{1}H}-CP-MAS NMR experiments (100.6 MHz) were recorded on a Bruker Digital Avance 400 spectrometer equipped with 7 mm double-tuned probes capable of MAS at 12 kHz. Data acquisition was performed with proton decoupling (TPPM). Spectra were referenced externally to tetramethyl silane (TMS) as well as to adamantane (δ = 38.48 ppm) as a secondary standard. ^{29}Si-{^{1}H}-CP-MAS NMR spectroscopy was performed at 79.5 MHz using 7 mm rotors spinning at 5 kHz. The contact time was 3 ms and the recycle delay 3 s. Shifts were referenced externally to tetramethylsilane (0 ppm) with the secondary standard being tetrakis(trimethylsilyl)silane (−9.8, −135.2 ppm). All spectra were collected with ^{1}H decoupling using a TPPM pulse sequence.

The FT-IR spectra were measured by means of diffuse reflection diluted with KBr at room temperature in the wavenumber range 400 to 4000 cm^{-1} on a Perkin-Elmer Fourier transform 1000 spectrometer. Elemental analysis was determined with a Vario-EL analyzer.

Crystal data were collected on a Oxford Gemini Diffractometer at low temperature (100 K) using Cu-K_α-radiation (λ = 1.54184 Å). The structure was solved by direct methods using SHELXS-97.[46] The structure was refined by full-matrix least-squares procedures on F^2 using SHELXL-97.[47] All non-hydrogen atoms were refined anisotropically. All hydrogen atoms were added to the calculated positions, except for OH and NH which were found by difference Fourier synthesis. For more details, see the Supporting Information.

Correlation Analysis. Multiple regression analysis (according Kamlet−Taft eq 1) was performed using the Origin 5.0 statistics program.

*Syntheses. {2-Nitro-4-[(E)-2-(4-nitrophenyl)vinyl]phenyl}propylamine **1-M**.* 1-Fluoro-2-nitro-4-[(*E*)-2-(4-nitrophenyl)vinyl]-benzene (**1**) (0.70 g, 2.429 mmol) was dissolved in toluene (40 mL) and *n*-propylamine (1.0 mL, 0.718 g, 12.144 mmol) was added in a single portion. The reaction mixture was heated for 10 h at 70 °C. Afterward the excess *n*-propylamine and solvent were distilled off. The solid red residue was crystallized from ethyl acetate to give the title compound as red crystals (75% yield). Mp 157−158 °C. ^{1}H NMR (250 MHz, DMSO-d_6, 25 °C): δ = 0.96 (3 H, t, ^3J = 7.4 Hz, CH$_3$), 1.58−1.73 (2 H, m, CH$_2$), 3.29−3.42 (2 H, m, CH$_2$), 7.13 (1 H, d, ^3J = 9.2 Hz, ArH), 7.27 (1 H, d, ^3J = 16.4 Hz, CH), 7.51 (1 H, d, ^3J = 16.4 Hz, CH), 7.80 (2 H, d, ^3J = 9.0 Hz, ArH), 7.92 (1 H, dd, ^3J = 9.2 Hz, ^4J = 2.1 Hz, ArH), 8.20 (2 H, d, ^3J = 9.0 Hz, ArH), 8.29 (1 H, d, ^4J = 2.1 Hz, ArH). ^{13}C NMR (69.9 MHz, DMSO-d_6, 25 °C): δ = 11.4, 21.9, 44.2, 115.5, 123.9, 124.2, 124.3, 125.8, 127.0, 130.8, 131.9, 134.2, 144.5, 145.4, 146.0. IR (KBr): $\tilde{\nu}$/cm^{-1} = 3366, 3075, 2932, 1625, 1588, 1512, 1333, 1242, 1199. Anal. Calcd for $C_{17}H_{17}N_3O_4$: C, 62.38; H, 5.23; N, 12.84. Found: C, 62.32; H, 5.18; N, 12.70. UV/vis: λ_{max}(MeOH)/nm 389 (ε/L mol^{-1} cm^{-1} 31200).

*(2S)-1-{2-Nitro-4-[(E)-2-(4-nitrophenyl)vinyl]phenyl}pyrrolidine-2-carboxylic acid **2**.* L-Proline (0.966 g, 8.655 mmol) and $NaHCO_3$ (0.145 g, 1.731 mmol) were dissolved in water (10 mL). To this solution was added 1-fluoro-2-nitro-4-[(*E*)-2-(4-nitrophenyl)vinyl]benzene (**1**) (0.499 g, 1.731 mmol) dissolved in acetone (40 mL) and water (10 mL). The reaction mixture was stirred for 72 h at room temperature and then poured into 2 M HCl (50 mL) in a single portion. The resulting pale red precipitate was recovered by filtration and washed with water. This material was purified by flash column chromatography (silica gel, diethyl ether, ethanol), affording **2** as a pale red solid (79% yield). Mp 130−132 °C. ^{1}H NMR (250 MHz, DMSO-d_6, 25 °C): δ = 1.84−2.03 (3 H, m, proH-3a, proH-4), 2.36−2.45 (1 H, m, proH-3b), 3.02−3.11 (1 H, m, proH-5a), 3.31−3.40 (1 H, m, proH-5b), 4.43−4.48 (1 H, m, proH-2), 6.94 (1 H, d, ^3J = 9.0 Hz, ArH), 7.30 (1 H, d, ^3J = 16.4 Hz, CH), 7.50 (1 H, d, ^3J = 16.4 Hz, CH), 7.78−7.81 (3 H, m, ArH), 7.99 (1 H, d, ^4J = 2.1 Hz, ArH), 8.21 (2 H, d, ^3J = 8.9 Hz, ArH), 12.90 (1 H, bs, COOH). ^{13}C NMR (69.9 MHz, DMSO-d_6, 25 °C): δ = 24.5, 30.5, 51.4, 61.8, 117.6, 124.3, 124.7, 125.2, 125.3, 127.1, 131.1, 131.6, 137.3, 141.3, 144.5, 146.0, 173.4. IR (KBr): $\tilde{\nu}$/cm^{-1} = 3078, 2981, 1716, 1589, 1520, 1337, 1189. Anal. Calcd for $C_{19}H_{17}N_3O_6$: C, 59.53; H, 4.47; N, 10.96. Found: C, 59.21; H, 4.59; N, 10.84. UV/vis: λ_{max}(DCM)/nm 390 (ε/L mol^{-1} cm^{-1} 27000).

*2-({2-Nitro-4-[(E)-2-(4-nitrophenyl)vinyl]phenyl}amino)propane-1,3-diol **3**.* 2-Amino-propane-1,3-diol (1.146 g, 12.578 mmol), $NaHCO_3$ (0.211 g, 2.512 mmol) and 1-fluoro-2-nitro-4-[(*E*)-2-(4-nitrophenyl)vinyl]benzene (**1**) (0.724 g, 2.512 mmol) were dissolved in acetone (50 mL). The reaction mixture was stirred for 72 h at 70 °C and then poured into water (50 mL). The resulting red precipitate was recovered by filtration and washed with chloroform, affording **3** as a red solid (82% yield). Mp 182 °C. ^{1}H NMR (250 MHz, DMSO-d_6, 25 °C): δ = 3.58−3.64 (4 H, m, CH$_2$), 3.79−3.86 (1 H, m, CH), 5.02 (2 H, t, ^3J = 5.7 Hz, OH), 7.25 (1 H, d, ^3J = 9.2 Hz, ArH), 7.31 (1 H, d, ^3J = 16.3 Hz, CH), 7.54 (1 H, d, ^3J = 16.4 Hz, CH), 7.82 (2 H, d, ^3J = 8.8 Hz, ArH), 7.95 (1 H, dd, ^3J = 9.2 Hz, ^4J = 2.1 Hz, ArH), 8.22 (2 H, d, ^3J = 8.8 Hz, ArH), 8.31 (1 H, d, ^4J = 2.1 Hz, ArH), 8.55 (1 H, d, ^3J = 8.4 Hz, NH). ^{13}C NMR (62 MHz, DMSO-d_6, 25 °C): δ = 55.6, 60.0, 116.2, 124.0, 124.3, 124.4, 135.9, 127.1, 130.9, 132.0, 134.1, 144.6, 145.5, 146.0. IR (KBr): $\tilde{\nu}$/cm^{-1} = 3324, 3226, 3074, 2943, 1626, 1588, 1506, 1338, 1290, 1213. Anal. Calcd for $C_{17}H_{17}N_3O_6$: C, 56.82; H, 4.77; N, 11.69. Found: C, 56.01; H, 4.64; N, 11.37. UV/vis: λ_{max}(MeOH)/nm 389 (ε/L mol^{-1} cm^{-1} 31200).

Preparation of Hybrid Precursors by the Sol−Gel Process. Reaction of 1-fluoro-2-nitro-4-[(*E*)-2-(4-nitrophenyl)vinyl]benzene (**1**) with aminopropylsilane (APS) and methylaminopropylsilane (MAPS), respectively, in tetraethoxysilane (TEOS): **1** and aminosilane were dissolved in TEOS (n_1:$n_{aminosilane}$:n_{TEOS} = 1:1:10) with stirring under an argon atmosphere. The mixture was heated to reflux for 5 h. An intense yellow color is developed in the course of the reaction and a nonviscous yellow solution is formed. After cooling the reaction solution to room temperature, the dark yellow solution was treated first with ethanol and then with distilled water. The amount of water added to initiate the sol−gel process is equimolar to the number of hydrolyzable

(46) Sheldrick, G. M. *Acta Crystallogr., Sect. A* **1990**, *46*, 467–473.
(47) Sheldrick, G. M. *SHELXL-97, Program for Crystal Structure Refinement*; University of Göttingen: Göttingen, Germany, 1997.

Scheme 2. Synthesis of Compounds 1-M, 2, and 3 by Nucleophilic Aromatic Substitution of Fluorostilbene 1 with *n*-Propylamine, L-Proline, and 2-Aminopropane-1,3-diol

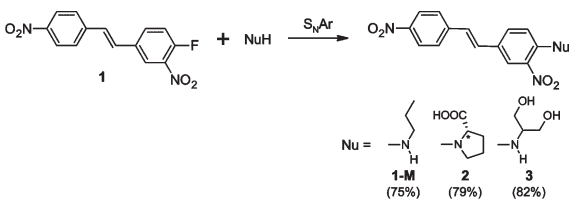

Si-OR groups ($n_{water} = 3n_{aminosilane} + 4n_{TEOS}$), with the reaction mixture being diluted in a 10-fold excess of ethanol compared to water prior to initiation ($n_{EtOH} = 10n_{water}$). When the gel had solidified, it was dried at 25 °C in vacuo and then unreacted **1** was removed by Soxhlet extraction with acetone. The xerogels **1a-XG** and **1b-XG** were then redried in vacuo.

The alkoxysilanes **2-XG** and **3-XG** containing the nitrostilbene unit were synthesized by a coupling reaction between 3-isocyanatopropyltriethoxysilane (ICPS) and a carboxylic acid- (**2**) and a diol-functionalized nitrostilbene (**3**), respectively. A multinecked flask was repeatedly evacuated and flushed with argon. Two precursors were placed in the flask with the solvent (THF). The mixture was stirred for several minutes and then refluxed in an oil bath for 48 h. After cooling to room temperature, TEOS (n_2:n_{ICPS}:n_{TEOS} = 1:1:10; n_3:n_{ICPS}:n_{TEOS} = 1:2:10) was added in a single portion to the resulting solution in THF. Aqueous acid (HCl, pH 1) was then added to promote the hydrolysis/condensation process. The amount of water added to initiate the sol−gel process is equimolar to the number of hydrolyzable Si-OR groups ($n_{water} = 3n_{aminosilane} + 4n_{TEOS}$). The solution was stirred at room temperature for 5 h and aged for 10 days to increase viscosity. When the gel had solidified, it was dried at 25 °C in vacuo and then unreacted chromophore was removed by Soxhlet extraction with acetone. The xerogels **2-XG** and **3-XG** were then redried in vacuo.

The surface modification of **1b-XG** was accomplished by allowing the hydroxyl groups on the dry gel surface to react with 20% HMDS, hexamethyldisilazane, in toluene for 5 h at 90 °C. Finally, the sample was washed with toluene to remove the unreacted surface modification agents and reaction products. The modified xerogel **1b-XG** was then redried in vacuo.

3. Results and Discussion

Synthesis and Characterization. The novel donor−acceptor-substituted stilbenes **1-M**, **2**, and **3** (Scheme 2) were obtained by nucleophilic aromatic substitution[48−55] of the activated fluoroaromatic **1**[33,34] with the corresponding amines.

Single-Crystal X-ray Analyses. Crystals of **1-M** and **3** suitable for single-crystal X-ray structure analysis were obtained by slow diffusion of *n*-hexane into an acetone solution of **1-M** and **3**, respectively. Compound **1-M** crystallizes in the orthorhombic space group *Pbca* and

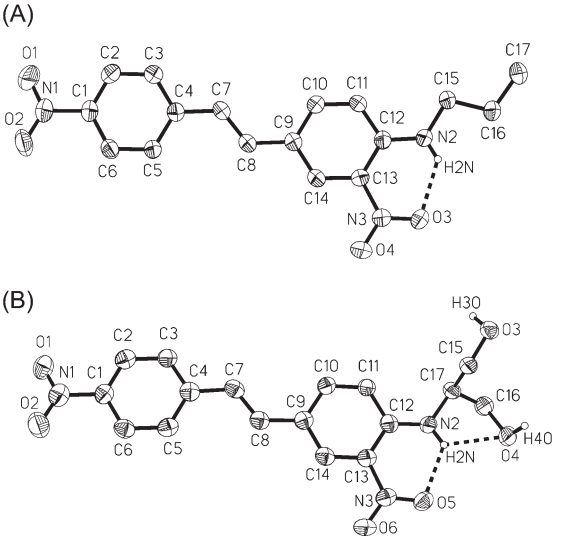

Figure 1. ORTEP diagrams of the molecular structure of (A) **1-M** and (B) **3**, respectively, with displacement ellipsoids shown at the 50% probability level. H-atoms, except OH and NH, are omitted for clarity.

the diol-functionalized stilbene **3** crystallizes in the monoclinic space group *P*2(1)/*n*. The molecular structures of both compounds are shown in Figure 1 together with the atomic labeling scheme. The crystallographic data, collection parameters, bond lengths (Å) and angles (deg) are provided as Supporting Information.

In the solid state, **1-M** and **3** possess a trans-configuration with respect to the central C=C double bond (C7−C8), as typically observed for stilbene compounds.[56] As expected,[57] there are intramolecular hydrogen bonds between the amino bonded hydrogen atoms and the ortho-nitro group (**1-M**: N2−H2N···O3, d = 2.621(2) Å, ∠ = 130(2)°; **3**: N2−H2N···O5, d = 2.624(4) Å, ∠ = 120(4)°). Additional, molecule **3** forms a further intramolecular hydrogen bond between the amino hydrogen and the hydroxyl oxygen atom (N2−H2N···O4, d = 2.778(4) Å, ∠ = 118(4)°). Compound **1-M** has no further functional groups except the nitro and the amino units and hence intermolecular hydrogen bonds are not observed. However, between two carbon atoms of two molecules (C12···C1A) of **1-M**, a very short distance is found (C12···C1A, d = 3.347 Å), obviously due to π−π interactions. Considering these interactions in the solid state, molecules of **1-M** are able to form a 2D layer along the crystallographic *b*- and *c*-axes (Figure 2).

In the solid state, a 3D network is obtained in the case of stilbene **3**. In contrast to **1-M**, it consists of 2D layers along the crystallographic *b*- and *c*-axes formed by intermolecular hydrogen bonds between the hydroxyl hydrogen atoms, the ortho-nitro group (O3A−H3OA···O6, d = 2.792(4) Å, ∠ = 172(3)°), and the diol groups (O4B−H4OB···O3A, d = 2.765(4) Å, ∠ = 169(4)°) (Figure 3), respectively. Because of π−π stacking interactions along the crystallographic *a*-axes between the ortho-nitro

(48) Bunett, J. F.; Zahler, R. E. *Chem. Rev*. **1951**, *49*, 273–412.
(49) Sauer, J.; Huisgen, R. *Angew. Chem*. **1960**, *9*, 294–315.
(50) Schmid, G. H. *Organic Chemistry*, 1st ed.; Mosby-Verlag: St. Louis, MO, 1996.
(51) Suhr, H. *Chem. Ber*. **1964**, *97*, 3277–3283.
(52) Suhr, H. *Liebigs Ann. Chem*. **1965**, *687*, 175–182.
(53) Suhr, H. *Liebigs Ann. Chem*. **1965**, *689*, 109–117.
(54) Suhr, H. *Chem.Ber*. **1964**, *97*, 3268–3276.
(55) Grube, H.; Suhr, H. *Chem. Ber*. **1969**, *102*, 1570–1579.
(56) Moran, A. M.; Bartholomew, G. P.; Bazan, G. C.; Meyers Kelley, A. *J. Phys. Chem. A* **2002**, *106*, 4928–4937.
(57) Panunto, T. W.; Urbánczyk-Lipkoswska, Z.; Johnson, R.; Etter, M. C. *J. Am. Chem. Soc*. **1987**, *109*, 7786–7797.

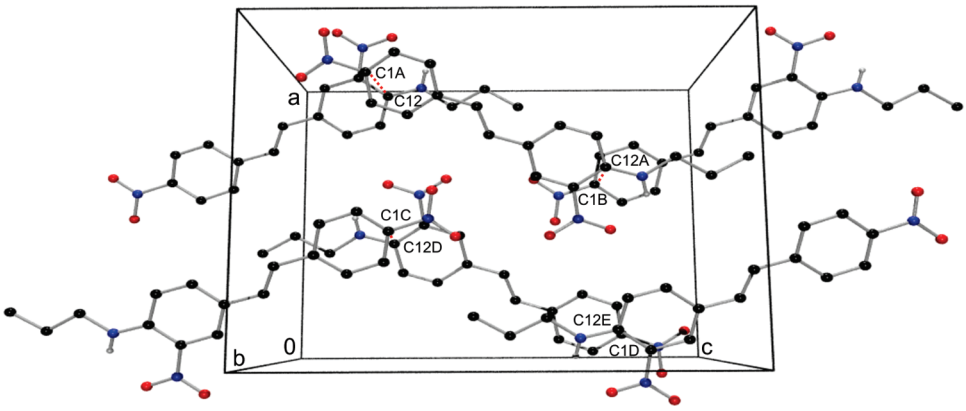

Figure 2. Part of the crystal packing of **1-M**. $\pi-\pi$ interactions are indicated with orange dotted lines.

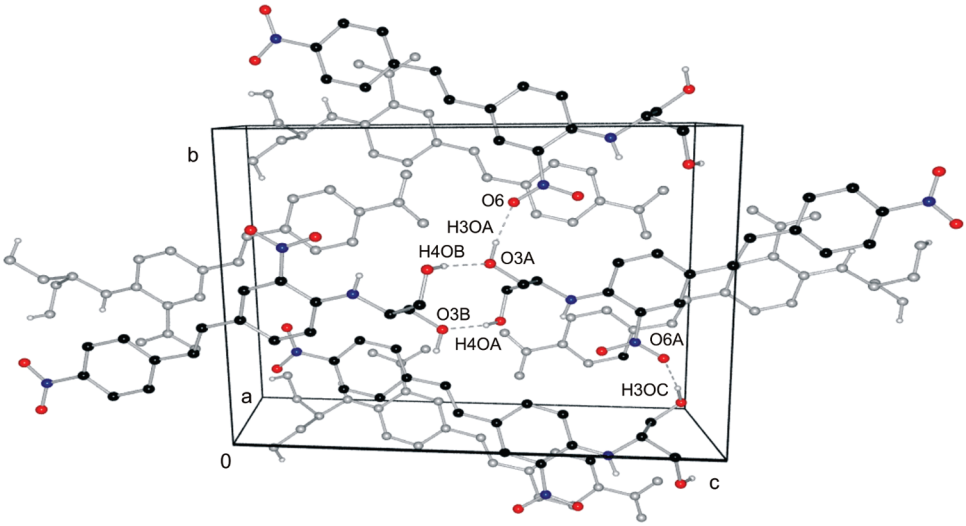

Figure 3. Selected part of the 3D network of **3** caused by intermolecular hydrogen bonds, indicated with dotted lines, displaying the alignment of one 2D layer. The gray molecules in the background represent a further 2D layer. The $\pi-\pi$ interactions between the nitro groups and the aromatic ring superimposed 2D layer are not illustrated here for clarity.

group and the aromatic unit (C1−C6), the 2D layers are connected to give a 3D network. A further graphical illustration of the 3D network is shown in Figure S1 in the Supporting Information.

Solvent Effects on the UV/Vis Absorption Spectra. The novel dyes **1-M**, **2**, and **3** (Figure 4) were investigated with respect to their activity as solvent-sensitive indicators.

The UV/vis absorption maximum of **2** in methanol shifts hypsochromically from $\tilde{\nu}_{max} = 407$ to 399 nm in a concentration range from 0.407×10^{-5} to 4.070×10^{-5} M. It is a fact that carboxylic acids form intermolecular hydrogen bonds and that the aggregation behavior is dependent on parameters such as acid concentration, temperature and solvent polarity.[58−63] Hence the solvatochromism of **2** is not investigated.

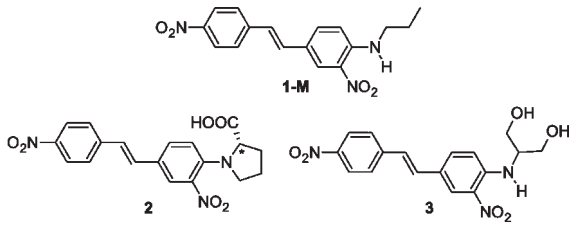

Figure 4. Chromophores **1-M**, **2**, and **3**.

Concentration-dependent UV/vis spectroscopic investigations of **1-M** and **3** did not show a shift in the UV/vis absorption maximum. The solvatochromic properties of compounds **1-M** and **3**, which do not undergo self-aggregation, can therefore be investigated (Table 1).

Compound **3** shows the shortest wavelength UV/vis absorption band at $\lambda_{max} = 383$ nm in tetrachloromethane, whereas **1-M** shows the strongest hypsochromic shift at $\lambda_{max} = 382$ nm in *n*-hexane, in which **3** is insoluble. For both chromophores, the longest wavelength UV/vis absorption maximum is observed at λ_{max}(**3**) = 415 nm, λ_{max}(**1-M**) = 412 nm in hexamethylphosphoramide (HMPA). These shifts correspond to a solvatochromic

(58) Schreiter, K.; Spange, S. *J. Phys. Org. Chem.* **2008**, *21*, 242–250.
(59) Bulmer, J. T.; Shurvell, H. F. *J. Phys. Chem.* **1973**, *77*, 256–262.
(60) Tanaka, N.; Kitano, H.; Ise, N. *J. Phys. Chem.* **1990**, *94*, 6290–6292.
(61) Laborie, F. *J. Polym. Sci.* **1977**, *15*, 1255–1274.
(62) Kuppens, T.; Herrebout, W.; Veken, B.; Bultnick, P. *J. Phys. Chem. A* **2006**, *110*, 10191–10200.
(63) Wolfs, I.; Desseyn, H. O. *J. Mol. Struct. (THEOCHEM)* **1996**, *360*, 81–97.

Table 1. UV/Vis Absorption Maxima of 1-M and 3 Measured in 36 Solvents of Different Polarity and Hydrogen-Bond Ability

	$\tilde{\nu}_{max}$ ($\times 10^3$ cm^{-1})	
solvent	**1-M**	**3**
cyclohexane	25.97	[a]
n-hexane	26.18	[a]
triethylamine	26.11	25.32
tetrachloromethane	25.71	26.11
p-xylene	25.45	25.58
toluene	25.45	25.58
benzene	25.38	25.58
diethyl ether	26.04	25.77
1,4-dioxane	25.51	25.51
anisole	25.00	25.06
tetrahydrofuran	25.32	25.13
ethyl acetate	25.58	25.45
chloroform	25.25	25.71
1,1,2,2-tetrachloroethane	24.88	25.13
pyridine	24.63	24.39
dichloromethane	25.13	25.45
hexamethylphosphoramide	24.27	24.10
tetramethylurea	24.75	24.51
1,2-dichloroethane	25.06	25.38
benzonitrile	24.69	24.63
acetone	25.32	25.38
N,*N*-dimethylacetamide	24.75	24.63
N,*N*-dimethylformamide	24.88	24.75
dimethyl sulfoxide	24.45	24.39
acetonitrile	25.32	25.44
nitromethane	25.13	25.06
1-decanol	25.58	25.25
1-butanol	25.51	25.38
2-propanol	25.77	25.45
1-propanol	25.58	25.45
ethanol	25.64	25.58
methanol	25.71	25.71
ethane-1,2-diol	24.75	25.06
formamide	24.63	24.69
2,2,2-trifluoroethanol	25.71	26.10
1,1,1,3,3,3-hexafluoro-2-propanol	25.19	25.84
$\Delta\tilde{\nu}$ (cm^{-1})	1906	2013

[a] Probe is insoluble in this solvent.

range of $\Delta\tilde{\nu}$(**3**) = 2013 cm^{-1} and $\Delta\tilde{\nu}$(**1-M**) = 1906 cm^{-1}, respectively.

LSE Correlation Analyses. The solvent-dependent UV/vis absorption of **1-M** and **3** can be interpreted with regard to the dipolarity/polarizability and hydrogen bonding capacity of the solvent using the Kamlet−Taft equation (eq 1).

The solvent parameters α, β, and π^* used for the multiple linear regression analysis are given in the Supporting Information. The qualitatively best regressions of **1-M** and **3** are shown in Table 2 as a function of the Kamlet−Taft solvent scale.

The correlation coefficient *r* is greater than 0.90 for LSE relationships, which indicates a high validity of the multiparameter equations and allows significant conclusions to be drawn. The most dominant effect on the solvatochromic behavior of compounds **1-M** and **3** is caused by interactions with solvents of different dipolarity/polarizability and is reflected in parameter *s*. The negative sign of *s* indicates that the electronically excited state of these molecules becomes stronger solvated and consequently stabilized with increasing the solvents dipolarity/polarizability. On the strength of the higher dipole moment, the energy of the electronically excited state decreases more than the ground state. This is well in agreement with a bathochromic shift of the UV/vis absorption maxima with increased polarity of the solvent.

For the nitrostilbene **3**, a negative correlation coefficient *b* is determined. On the other hand, hydrogen-bond acceptor (HBA) solvents do not have any effect on the position of the UV/vis absorption maximum of **1-M** ($b = 0$). For **1-M**, interactions between the NH-function and HBA solvents are merely conceivable ($b < 0$). However, this interaction competes with the formation of an intramolecular hydrogen bond to the ortho-nitro group[64] ($b = 0$). Compound **3** can also form an intramolecular hydrogen bond as observed for **1-M**. Solvents with HBA ability can also interact with **3** via specific solvation of the diol group.[65] This result is initially surprising, because the diol function is separated from the aromatic push−pull system by the propyl group spacer. However, this is confirmed by the results of the linear multiple regression analysis of **1-M**. Furthermore, we found a similar effect on the β-parameter in solvatochromic investigations on *N*-(2-hydroxyethyl)-substituted Michlers ketone and *N*-(methyl-*N*-[1-(2,3-dihydroxypropyl)]-4-nitroaniline derivatives.[66−68]

The positive sign of parameter *a* for **1-M** and **3** indicates that there is a hypsochromic shift of λ_{max} with increasing hydrogen-bond donor capacity of the solvent (negative solvatochromism). This suggests that the ground state is more stabilized than the first excited state. This can be explained in terms of a possible interaction with the free electron pair of the nitrogen or the amino function.

Preparation of Chromophoric Class II Xerogels. Starting from the nitrostilbenes **1**−**3**, we prepared organofunctionalized class II silicate-based xerogels by the combination of first nucleophilic aromatic substitution (Ia), amide formation (Ib), or urethane formation (Ic) and a subsequent sol−gel process (II) in tetraethoxysilane (TEOS) in a one-pot synthesis (Scheme 3, Table 3).

The advantage of the one-pot syntheses of **1a-XG** and **1b-XG** is the use of TEOS as solvent and cross-linking agent in the sol−gel process, which is a key feature of this synthesis route. The advantage of the two-step synthesis route for **2-XG** and **3-XG** is the possibility to vary the linker between the chromophore and the silicate network and thus allow the incorporation of tailor-made organic components.

A summary of the xerogel syntheses carried out and the characterization of the xerogels **1-XG**−**3-XG** obtained is given in Table 3. To obtain **1-XG** and **2-XG** a 1:1:10 n_C:n_{TAS}:n_{TEOS} molar ratio was used. Because of the two hydroxyl functionalities in **3**, a 1:2:10 n_3:n_{TAS}:n_{TEOS} molar ratio was used for **3-XG**, incorporating the chromophoric building block in the main chain of the silica

(64) Cattana, R.; Silber, J. J.; Anunziata, J. *Can. J. Chem.* **1992**, *70*, 2677–2682.
(65) Spange, S.; Hofmann, K.; Walfort, B.; Rüffer, T.; Lang, H. *J. Org. Chem.* **2005**, *70*, 8564–8567.
(66) El-Sayed, M. M.; Müller, H.; Rheinwald, G.; Lang, H.; Spange, S. *J. Phys. Org. Chem.* **2001**, *14*, 247–255.
(67) Spange, S.; El-Sayed, M. M.; Müller, H.; Rheinwald, G.; Lang, H.; Poppitz, W. *Eur. J. Org. Chem.* **2002**, 4159–4168.
(68) El-Sayed, M. M.; Müller, H.; Rheinwald, G.; Lang, H.; Spange, S. *Chem. Mater.* **2003**, *15*, 746–754.

Table 2. Solvent-Independent Correlation Coefficients *a*, *b*, and *s* of the Kamlet−Taft Parameters α, β, and π^*; Solute Property of the Reference System $\tilde{\nu}_{max,0}$, Significance (*f*), Correlation Coefficient (*r*), Standard Deviation (sd), and Number of Solvents (*n*) Calculated for the Solvatochromism of 1-M and 3

eq	compd	$\tilde{\nu}_{max,0}$	*a*	*b*	*s*	*n*	*f*	*r*	*sd*
1	**1-M**	26.262 (±0.091)	0.182 (±0.070)	0	−1.641 (±0.131)	36	< 0.0001	0.911	0.205
1	**3**	26.515 (±0.125)	0.348 (±0.069)	−0.849 (±0.109)	−1.490 (±0.157)	34	< 0.0001	0.925	0.197

Scheme 3. One-Pot Synthesis of Chromophoric Sol−Gel Hybrid Materials (Class II) 1-XG−3-XG: Nucleophilic Aromatic Substitution (Ia), Amide Synthesis (Ib), and Urethane-Forming Reaction (Ic), Followed by Sol−Gel Processing (II)

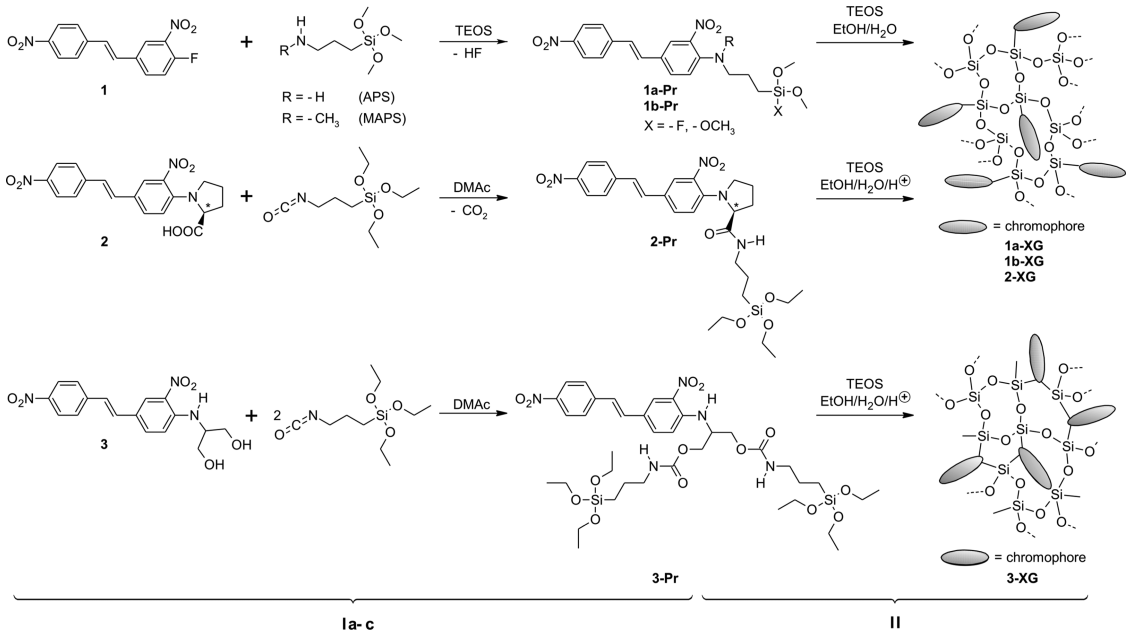

Table 3. Experimental Conditions and Characterization of 1-XG−3-XG

chromophore (C)	trialkoxy-silane (TAS)	n_C:n_{TAS}:n_{TEOS} ratio		results				
				λ_{max} (nm)	BET (m^2/g)	T_d[a] (°C) via DSC	T_g[b] (°C) via DSC	T_d[c] (°C) via TGA
1	APS	1:1:10	**1a-XG**	392	114	269	93	213
	MAPS	1:1:10	**1b-XG**	392	52	230	85	247
2	ICPS	1:1:10	**2-XG**	383	127	242	89	241
3	ICPS	1:2:10	**3-XG**	393	40	275	89	216

[a] T_d = Onset decomposition temperature of chromophore incorporated in silica network. [b] T_g = Glass transition temperature. [c] T_d = Decomposition temperature where there is 5 wt % loss under nitrogen.

network. The covalent bonding of the organic dye molecule in an inorganic matrix can occur in various ways. The surface areas of the xerogels were determined by the BET method (Table 3). A low surface area was found for all xerogels under study.

FT-IR Spectra. The successful incorporation of the nitrostilbene unit into a silica network via various linkers could be established using FTIR spectroscopy. The FTIR spectra of **1-M**, **2**, and **3** and their corresponding xerogels (**1-XG**−**3-XG**) each exhibit two sharp absorption bands in the range of 1506−1530 and 1333−1341 cm^{-1}, respectively, which correspond to the asymmetric and symmetric stretching vibrations of the nitro group of the chromophoric building block. Furthermore, for the carboxylic-acid-functionalized stilbene **2** a $\nu_{C=O}$ absorption at 1716 cm^{-1} is observed. After conversion into the xerogel (**2-XG**), this band is, as expected, no longer observed. Instead a $\nu_{C=O}$ stretching vibration at 1688 cm^{-1} corresponding to the amide group appears. The FTIR spectrum of the diol-substituted nitrostilbene **3** shows typical −OH and −NH stretching vibrations between 3400−3200 cm^{-1}. The corresponding xerogel **3-XG** shows stretching vibrations at 3352 and 1702 cm^{-1} (ν_{N-H} and $\nu_{C=O}$), which are evidence of urethane formation. In all xerogels **1-XG**−**3-XG**, a strong absorption band is seen in the range of 1200−1000 cm^{-1} corresponding to the Si−O−Si stretching vibrations.

Glass-Transition Temperatures. The glass transition temperature (T_g) is an important parameter for determining the stability of dipolar orientations of chromophores in a matrix. T_g can be affected by various factors such as the degree of cross-linking, the size of the chromophore and the ratio of reactants used.[69] For our synthesis we

(69) Silva, S. S.; Ferriera, R. A. S.; Fu, L.; Carlos, L. D.; Mano, J. F. R.; Reis, L.; Rocha, J. *J. Mater. Chem.* **2005**, *15*, 3952–3961.

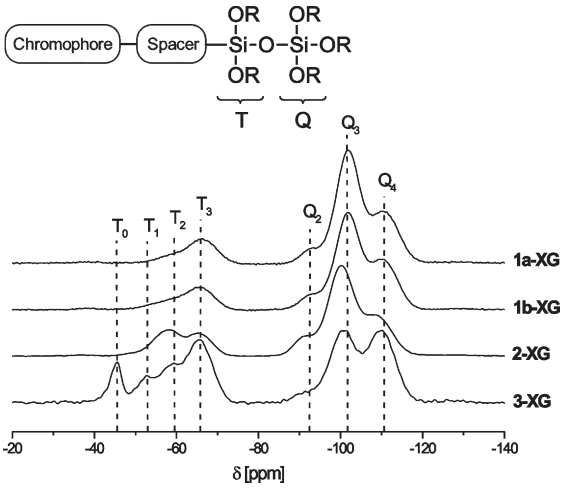

Figure 5. ^{29}Si-{^{1}H}-CP-MAS NMR spectra of xerogels **1-XG**−**3-XG** (nomenclature, see Scheme 2).

always chose the same chromophoric building block and similar molar ratios of the reactants, thus obtaining hybrid materials with T_g in the relatively narrow range of 85−93 °C (Table 1). These data were determined by differential scanning calorimetry (DSC).

Thermal Stability. The thermal stability of the hybrid materials obtained was determined by thermogravimetric analysis under an inert gas atmosphere (Table 3). The results of the TGA show that the onset of decomposition of xerogels with a secondary amine function as the structural element begins in a similar temperature range: **1a-XG** T_d = 213 °C, **3-XG** T_d = 216 °C. The initial decomposition temperature for **1b-XG** (T_d = 247 °C) and **2-XG** (T_d = 241 °C), which have a tertiary amine function as the structure-forming building block, is about 30 °C higher in each case.

^{29}Si-{^{1}H}-CP-MAS NMR Spectroscopy. ^{29}Si-{^{1}H}-CP-MAS NMR spectra of the xerogels **1-XG**−**3-XG** were recorded (Figure 5). Using cross-polarization, qualitative spectra with good signal-to-noise ratios could be obtained within a short time. However, only the presence of the individual signals can be used as reliable evidence; the intensity ratios of the individual signals do not correspond to the actual concentrations in the xerogel. The ^{29}Si-{^{1}H}-CP-MAS NMR spectrum of **1-XG**−**3-XG** confirmed the covalent bonding of the organic moiety to the matrix by the appearance of T_2 and T_3 signals due to the ligand in addition to the characteristic Q_3 and Q_4 signals due to condensed TEOS. ^{29}Si-{^{1}H}-CP-MAS NMR spectrum of **1a-XG** shows five signals. The signals at $\delta = -66.3$ ppm (T_3) and $\delta = -58.9$ ppm (T_2) arise from the trialkoxysilane component, which is embedded into the silicate matrix. The signals at $\delta = -110.0$ ppm (Q_4), $\delta = -101.8$ ppm (Q_3), and $\delta = -93.6$ ppm (Q_2) can be assigned to the silanol groups and siloxane bridges in the silicate matrix. In the ^{29}Si-{^{1}H}-CP-MAS NMR spectra of the networks **1b-XG** and **2-XG**, besides the Q_4 signal, as in **1a-XG**, there are Q_3 and Q_2 signals arising from tetraethoxysilane, which is hydrolyzed and condensed partially. The T_3 signal and a small shoulder of very low intensity for the T_2 signal can also be seen.

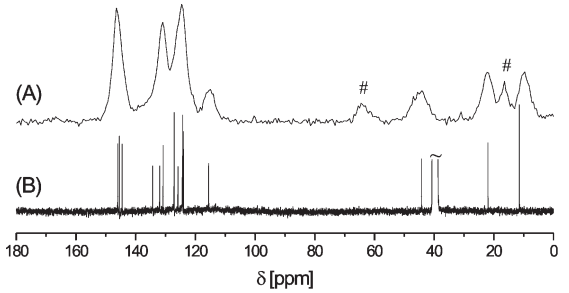

Figure 6. (A) Solid state ^{13}C-{^{1}H}-CP-MAS NMR spectra of xerogels **1a-XG** (12.5 kHz MAS frequency); (B) ^{13}C-{^{1}H} NMR spectrum of **1-M** (DMSO-d_6). The rhomb (#) indicates unhydrolyzed ethoxy groups in the xerogel.

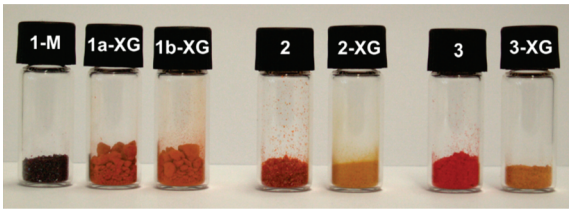

Figure 7. Photograph of stilbenes **1-M**, **2**, **3**, and their xerogels **1-XG**−**3-XG**.

1b-XG: −109.4 (Q_4), −101.8 (Q_3), −93.5 (Q_2), −65.4 (T_3), −59.2 (T_2); **2-XG**: −107.5 (Q_4), −100.2 (Q_3), −92.5 (Q_2), −65.3 (T_3), −58.1 (T_2). For **3-XG**, T_0 (−45.6) and T_1 (−52.7) signals can also be observed in the ^{29}Si-{^{1}H}-CP-MAS NMR spectrum, besides T_2 (−59.3) and T_3 (−65.7) signals. The T_0 signal can be assigned to the 3-isocyanatopropyltriethoxysilane (ICPS)[70] or the precursor **3-Pr**. However, the completely unreacted educts (ICPS, **3-Pr**) should be removed by Soxhlet extraction. A T_0 signal is also observable in the case that only one of these two groups is bound to the silica matrix and the other one remains unhydrolized. However, under the current conditions of measurement, the intensity ratios of ^{29}Si signals, e.g., T_0, do not correspond to the actual concentrations in the xerogel.

^{13}C-{^{1}H}-CP-MAS NMR Spectroscopy. In Figure 6, the ^{13}C-{^{1}H}-CP-MAS NMR spectrum of **1a-XG** (A) and the ^{13}C-{^{1}H} NMR spectrum of **1-M** (B) measured in DMSO-d_6 is depicted. On comparison of these spectra, it can be seen that the resonances observed for **1-M** are also visible in the ^{13}C-{^{1}H}-CP-MAS NMR spectrum of **1a-XG**. This is evidence for the integrity of the chromophoric building block even after incorporation into the class II xerogel. Furthermore, the spectrum has two further signals at 16.4 and 64.3 ppm due to the nonhydrolyzed Si−OEt groups. These results are in agreement with those from the ^{29}Si-{^{1}H}-CP-MAS NMR spectroscopy (Q_3 and Q_2 signals).

UV/Vis Reflection Spectra. The class II xerogels **1-XG**−**3-XG** obtained have orange to orange-red color shades (Figure 7). An interesting application for these types of chromophores, incorporated in an inorganic matrix, may be in the area of substantial pigments.

(70) Lebeau, B.; Maquet, J.; Sanchez, C.; Toussaere, E.; Hierle, R.; Zyss, J. *J. Mater. Chem.* **1994**, *4*, 1855–1860.

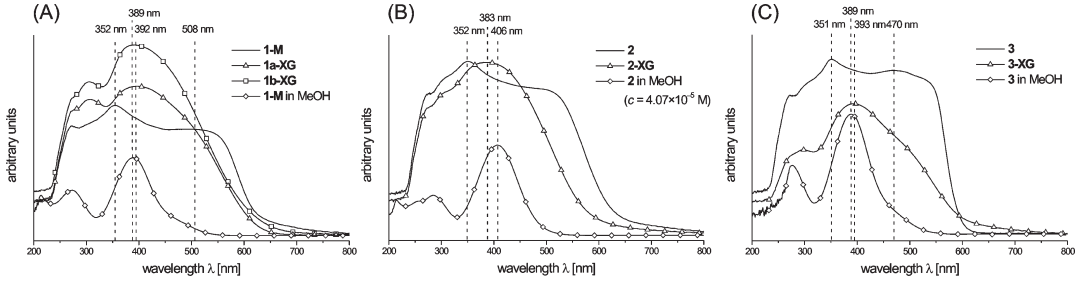

Figure 8. UV/vis absorption spectra of (A) **1-M**, (B) **2**, (C) **3**, and their xerogels **1-XG**−**3-XG**, respectively, as solid powders and dissolved in methanol.

UV/vis absorption spectra of class II xerogels **1-XG**−**3-XG** have been measured by means of diffuse reflectance spectroscopy. The polarity in terms of the $E_T(30)$ scale of non chromophoric derivatized amino-xerogel ($E_T(30)$ = 55 kcal/mol) is close to that of methanol ($E_T(30)$ = 55.4 kcal/mol).[71] Referring to $E_T(30)$ values in the same order of magnitude, protonation of the probe at both the nitro group oxygen and the amino group nitrogen atom can not be expected. Representative UV/vis spectra of **1-XG**−**3-XG**, and **1-M**, **2**, and **3**, measured as powders and dissolved in methanol for comparison are shown in Figure 8A−C. Generally, the half-with of the UV/vis absorption band of the respective xerogels are broader than those in well-behaved regular solvents, e.g., methanol. This result indicates a wider polarity distribution compared to that of a solvent.

The UV/vis absorption bands are nonsymmetric and show several UV/vis absorption maxima. The UV/vis diffuse reflectance spectra of the xerogels **1-XG**−**3-XG** exhibit UV/vis absorption maxima at 392 nm (**1-XG**, **3-XG**) and 383 nm (**2-XG**). For the corresponding nitrostilbenes **1-M**, **2**, and **3** a distinct UV/vis absorption maximum at 352 nm is present.

In the solid state the chromophores **1-M**, **2**, and **3** form intra- and intermolecular hydrogen bonds in addition to strong dipolar interactions. This is verified by the single crystal X-ray structures of **1-M** and **3**. The directed specific intermolecular interaction between the nitro group oxygen and one HBD moiety (specifically observed for **3**) causes a significant bathochromic UV/vis shift. As the chromophore is encapsulated by the silica network (**1-XG**−**3-XG**), the formation of dipolar interactions between the chromophores is limited. This can be the explanation for the fact that the width of the UV/vis reflection bands of the stilbenoid building blocks is clearly broader than that of the corresponding xerogels.

The treatment of **1b-XG** with hexamethyldisilazane (HMDS) leads to a replacement of the surface hydroxyl groups by trimethylsilyloxy groups, resulting in a decrease in the acidity of the xerogel surface. Furthermore, a decrease in the term dipolarity/polarizability occurs. From the results of the Kamlet−Taft analysis of **1-M** and **3**, it can be concluded that the influence of changes in the dipolarity/polarizability on the UV/vis behavior of **1b-XG** is more dominant than variations of surface acidity. The UV/vis absorption maximum of the trimethylsilyl modified **1b-XG** is shifted to slightly higher energies ($\Delta\tilde{\nu}$ = 330 cm^{-1}) in comparison to the unmodified material. This observation is in agreement with the solvatochromic study.

4. Conclusion

We have presented a series of variously functionalized nitrostilbenes (**1-M**, **1**−**3**). In the solid state, the chromophores **1-M**, **2**, and **3** form intra- and intermolecular hydrogen bonds in addition to strong dipolar interactions. This is verified by the single crystal X-ray structures and UV/vis diffuse reflectance spectroscopy of **1-M** and **3**. A comprehensive study of the solvent effects on the position of the wavelength absorption band of **1-M** and **3** is presented. The absorption maxima have been measured in a variety of HBD and non-HBD solvents. Overall, the two nitrostilbenes show a positive solvatochromism and a solvatochromic range of $\Delta\tilde{\nu}$(**3**) = 2013 cm^{-1} and $\Delta\tilde{\nu}$(**1-M**) = 1906 cm^{-1}, respectively. The result of such correlations suggests that the influence of solvent dipolarity/polarizability on the long wavelength absorption maximum for **1-M** and **3** is more predominant. The functionalization of nitrostilbenes **1**−**3** allows reaction with trialkoxysilanes to give the chromophoric trialkoxysilanes **1-PR**−**3-PR**, which were converted into the corresponding organically modified class II silica gels (**1-XG**−**3-XG**). Structural characterization by a range of techniques (FT-IR, ^{29}Si-CP-MAS NMR, ^{13}C−CP-MAS NMR, thermogravimetric analysis) confirmed that class II hybrid materials are available. The absence of T_0 signals in **1-XG**−**2-XG** shows that unreacted precursor is not present in the materials obtained. However, a T_0 signal observed for **3-XG** is originated by one of two possible triethoxysilyl groups from **3-Pr**. All materials obtained show similar thermal behavior.

In such xerogels, the formation of dipolar interactions between the chromophores is limited in comparison to the pure chromophores.

Acknowledgment. Financial support from the Deutsche Forschungsgemeinschaft and the Fonds der Chemischen Industrie is gratefully acknowledged. The authors thank R. Lungwitz, P. Schönherr, and R. Jaeschke, Department of Polymer Chemistry, Chemnitz University of Technology, for solid-state NMR, TGA, and DSC measurements.

(71) Seifert, A.; Spange, S.; Müller, H.; Hesse, S.; Jäger, C *J. Sol*−*Gel Sci. Technol.* **2003**, *26*, 77–81.

Supporting Information Available: Crystal data for **1-M** and **3** have been deposited with the Cambridge Crystallographic Data Center as supplementary publication no. 745588 and no. 745589. Copies of this information can be obtained free of charge on application to CCDC, 12 Union Road, Cambridge CB2 1ET, UK. Kamlet−Taft parameter set, all results of the multiple linear regression analyses, X-ray crystallographic data, collection parameters of **1-M** and **3** (PDF). This material is available free of charge via the Internet at http://pubs.acs.org.